FARADAY

Vibrational spectra and computer simulations of ^{18}O-labelled NaY zeolites

Ekkehard Geidel,[a]*† Knut Krause,[a] Horst Förster[a] and Frank Bauer[b]

[a] *Institute of Physical Chemistry, University of Hamburg, Bundesstrasse 45, 20146 Hamburg, Germany*

[b] *Institute of Analytical Chemistry, University of Leipzig, Permoserstrasse 15, 04303 Leipzig, Germany*

The Raman, mid- and far-IR spectra of NaY and ^{18}O-labelled NaY are presented and compared with spectra calculated by a shell model and by a simple valence force field. The calculations of the kinetic-energy distribution (KED) and the potential-energy distribution (PED) were used to assign experimentally observed bands to normal modes.

Vibrational spectroscopic techniques, *e.g.* IR, Raman and inelastic neutron scattering (INS) spectroscopy, have proven to be valuable tools for the characterization of microporous materials.[1,2] Nevertheless, the successful analytical application of these methods needs reliable assignments of the observed fundamentals to the individual normal modes. In the case of zeolites, a straightforward interpretation of the spectral data is a difficult task owing to the complexity of zeolite frameworks which contain large numbers of atoms per unit cell. The crystal symmetry for given structure types is also determined by the silicon/aluminium ratio and is usually low for zeolites of chemical interest. On the other hand, the vibrational spectra of zeolites are mostly characterized by only a limited number of broad, strongly overlapped bands. In this situation, isotope exchange can be helpful to gain additional information. Whereas isotopic labelling is a routine procedure in spectroscopic studies of organic molecules, in the field of zeolites only the H/D exchange of hydroxy groups is a well established technique for IR and INS investigations. Studies by isotopic substitution of framework atoms are scarce. The aim of this study is to obtain more detailed knowledge on the vibrational behaviour of NaY by comparing the IR and Raman spectra of common NaY and ^{18}O-exchanged NaY.

Aside from the progress in the development of experimental methods the use of modelling techniques provides a deeper insight into molecular properties. Therefore, during the last years, various efforts have been made to understand the vibrational spectra of zeolites on the basis of computational methods such as quantum mechanics, molecular dynamics (MD) and molecular mechanics (MM) and normal coordinate analyses (NCA).[3–5] Not only IR and Raman spectra can be simulated, but also normal modes can be characterized by energy distributions and atomic displacements, often called eigenvectors, enabling the alignment of experimentally observed bands to individual normal modes. However, in the case of force field methods there are often insufficient experimental data to generate reliable empirical potential functions. Isotope exchange is one way to get a more comprehensive experimental data basis. Furthermore, this method is useful to verify the physical relevance of a force field under study.

The aim of our study with respect to modelling techniques is twofold. First, we should like to get a deeper insight into the vibrational behaviour of NaY by calculation of the potential- and kinetic-energy distributions. Second, we would like to test given valence and ionic force fields in order to describe the experimentally obtained isotopic shifts correctly. The accurate description of experimentally obtained isotopic shifts is an important criterion of the physical relevance of the force field under study.

† E-mail: geidel@chemie.uni-hamburg.de

Experimental

NaY zeolite with a Si/Al ratio of 2.6 and a unit-cell composition $Na_{53.3}[Al_{53.3}Si_{138.7}O_{384}]$ was treated with $H_2{}^{18}O$ vapour (98% ^{18}O, Chemotrade, Germany) at 620 K for 1 h in a nitrogen flow. As shown by von Ballmoos[6] for ZSM-5, this procedure yields *ca.* 70% oxygen isotopic exchange, while no change in the Si/Al ratio, as a result of the hydrothermal treatment, is observed. Because the vibrational spectra of ^{18}O-ZSM-5 revealed comparable shifts[7] a similar degree of exchange has to be assumed in the case of zeolite NaY.

Wafers containing 1 mg zeolite and 20 mg KBr were mounted in a vacuum cell equipped with potassium bromide windows. The samples were activated *in vacuo* for 2 h at 670 K. Mid-IR spectra were recorded in the 4000–400 cm^{-1} range using a Digilab FTS 20E spectrometer with a resolution of 2 cm^{-1}, accumulating 1024 scans.

In order to record far-IR spectra, self-supporting wafers of the pure samples were inserted in a cell furnished with polyethylene windows. After dehydration at 670 K in a stream of dry nitrogen and cooling to room temperature, far-IR spectra were recorded in the 400–20 cm^{-1} range co-adding 256 scans at a resolution of 4 cm^{-1}. The Digilab FTS 15E spectrometer was equipped with a mercury vapour source and a liquid-helium-cooled silicon bolometer (Infrared Laboratories) as a high sensitivity detector.

Raman spectra of the zeolite powders as such were obtained on a Perkin–Elmer System 2000R NIR-FT Raman spectrometer using an Nd-YAG laser with wavelength 1064 nm and power 450 mW.

Computational procedure

Vibrational spectra were calculated using two different approaches. The first is a lattice energy minimization at constant pressure followed by eigenvalue calculation in Cartesian coordinates, employing the METAPOCS code.[8] The force field is based on the shell model[9] consisting of four types of potentials.

The electrostatic interaction of all cores and shells are calculated with a Coulomb potential where r_{ij} is the distance of the point charges q_i and q_j.

$$E^{\text{Coulomb}} = \sum_{i,j} \frac{q_i q_j}{r_{ij}} \quad (1)$$

The long-range Coulomb interaction is computed using the Ewald summation technique.[10] In order to take into account the polarizability of oxygen and sodium ions, the interaction between core and shell at the distance R_i is described by a harmonic potential

$$E^{\text{core–shell}} = \sum_i K_i R_i^2 \quad (2)$$

whereas silicon and aluminium atoms are treated as rigid. The short-range interactions are taken into account by a Buckingham-potential eqn. (3) neglecting the dispersion term by setting the constants C_{kl} equal to zero. This type of potential is known as the Born–Mayer potential[11] with the empirical parameters A_{ij} and ρ_{ij} using 10 Å as short-range cut-off.

$$E^{\text{repulsion}} = \sum_{k,l} A_{kl} \exp\left(-\frac{r_{kl}}{\rho_{kl}}\right) - \sum_{k,l} \frac{C_{kl}}{r_{kl}^6} \quad (3)$$

The stiffness of the tetrahedron angles is described by a harmonic three-body-potential

$$E^{\text{three-body}} = \frac{1}{2} \sum_l \sum_{m,n} k_l(\theta_{lmn} - \theta_0)^2 \quad (4)$$

The indices m and n run over all oxygen atoms connected to the atom l.

The force-field parameters describing silicon, aluminium and oxygen atoms are taken from Schröder and Sauer.[12] Since no parameters for extra-framework cations are given, the parameters for sodium ions were obtained from the Biosym implementation of METAPOCS.[13] All values are given in Table 1.

The primitive unit cell containing one double sodalite unit with 96 oxygen, 36 silicon, 12 aluminium and 12 sodium ions (Fig. 1) was used as the simulation box under periodic boundary conditions. The initial coordinates were taken from Olson.[14] After energy minimization, frequencies and normal modes were obtained by an eigenvalue calculation. The normal modes were used to compute IR intensities applying the procedure described by Creighton *et al.*[15] implemented in our own code. To simulate spectra, a full width at half height was assumed to be 60 cm^{-1} in the mid-IR and 20 cm^{-1} in the far-IR range.

Table 1 Parameters of the shell-model calculations

charge, q_i	core/e	shell/e
Si	4.0	—
Al	3.0	—
O	1.06237	−3.06237
Na	−1.13	2.13
core-shell potential	K_i/eV Å^{-2}	
O	112.7629	
Na	96.44	
repulsion potential	A_{ij}/eV	ρ_{ij}/Å
Si—O	1550.950	0.30017
Al—O	1068.711	0.32260
Na—O	1226.84	0.3065
Na—Na	7895.4	0.1709
three-body potential	k_{lmn}/eV rad^{-2}	θ_0/grad
O—Si—O	0.18397	109.47
O—Al—O	0.64984	109.47

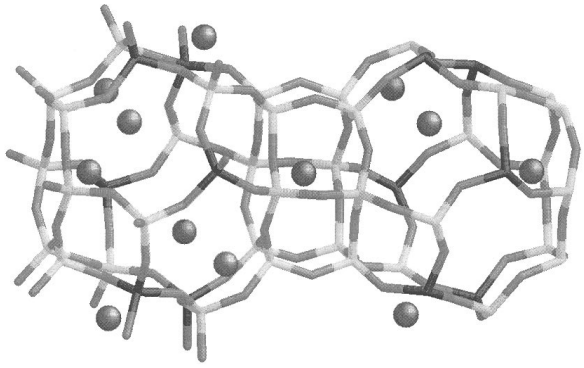

Fig. 1 Primitive unit cell of sodium faujasite. Silicon atoms are drawn in light grey, aluminium atoms in dark grey and sodium ions are spheres.

Even if bonding in zeolite frameworks has a significant ionic contribution, the purely ionic treatment of bond stretchings within the shell model often gives larger deviations from experiment in the range of framework stretching modes.[16,17] Thus, in a second approach, calculations on the basis of a valence force field were carried out. For this, normal coordinate analyses were performed by means of Wilson's GF matrix method[18] in internal coordinates using the Jones program package.[19] The so-called bond length scaled force field on the basis of Badger's rule (BLSF-BR) was adopted. This force field was originally developed by Blackwell[20] and later widely applied in normal mode analyses of zeolite subunit cluster models.[21,22] The complete internal valence force field (IVFF) is described by the potential function

$$V = \frac{1}{2}\sum_i F_{ii}^r(\Delta r_i)^2 + \frac{1}{2}\sum_k r_0^2 F_{kk}^\alpha(\alpha_k)^2 + \frac{1}{2}\sum_{i\neq j} f_{ij}^{rr}(\Delta r_i)(\Delta r_j) + \frac{1}{2}\sum_{k\neq l} r_0^2 f_{kl}^{\alpha\alpha}(\Delta\alpha_k)(\Delta\alpha_l) + \frac{1}{2}\sum_{i,k} r_0 f_{ik}^{r\alpha}(\Delta r_i)(\Delta\alpha_k) \quad (5)$$

with $r_{i,j}$ = atomic distances along chemical bonds, $\alpha_{k,l}$ = bond angles (in plane, out of plane and torsional ones), F^r = stretching, F^α = bending and f = interaction force constants (all in N m^{-1}).

In the BLSF-BR, only the first two terms, which include the diagonal force constants, are taken into account. Similar to the first approach, the model consists of a double sodalite unit. As no periodic boundary conditions were used, all terminating O(1) oxygen atoms were included to realize a tetrahedral environment for all T atoms with oxygen. Since the force field implies only covalent bonds, cations were completely ignored. In this way a cluster model of 162 framework atoms was built up.

The spectra were generated from the calculated frequencies assuming a Gaussian band shape with a full width at half height of 50 cm^{-1}. Since no explicit calculation of IR intensities was performed, a simple intensity weighting factor of 0.5 was assumed in the region below 700 cm^{-1}, as the number of bending modes in this range is twofold larger per frequency interval than the number of stretchings above 700 cm^{-1}.

The force constants are known to be independent of the isotopic mass, *e.g.* the same force field has to be used for calculating ^{16}O and ^{18}O spectra. Thus, the isotopic exchange is an additional test for the physical relevance of a force field.

Results and Discussion

Experimental spectra

The experimental IR spectra of sodium faujasite and the ^{18}O-labelled sample are shown in Fig. 2 and 3, the corresponding Raman spectra are given in Fig. 4. Wavenumbers of observed

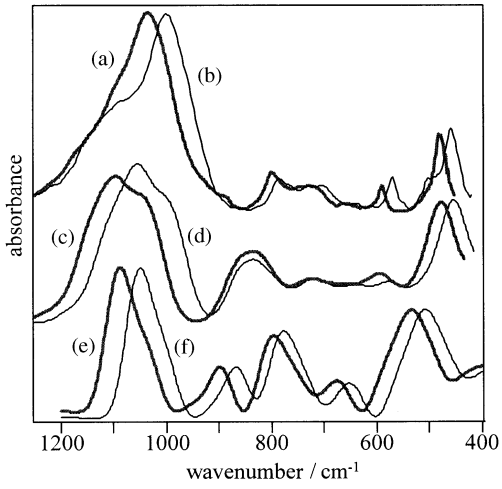

Fig. 2 Mid-IR spectra: experimental NaY (a) and ^{18}O-NaY (b), shell model calculated NaY (c) and ^{18}O-NaY (d), VFF calculated NaY (e) and ^{18}O-NaY (f)

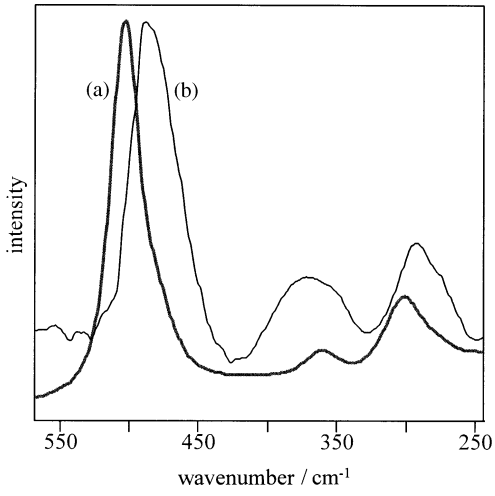

Fig. 4 Experimental Raman spectra of NaY (a) and ^{18}O-NaY (b)

and calculated bands are summarized in Table 2. Under the exchange conditions described in the Experimental section, no indications for lattice defects were observed. As can be seen, no additional bands occur in the spectra of the ^{18}O-exchanged samples, but some bands become more structured, in particular, the shoulders at 1088 and 502 cm^{-1}. In all spectra, shifts to lower wavenumbers due to ^{18}O exchange are observed, but the extent of the displacement is different in different spectral regions. The largest shifts, up to 33 cm^{-1} downscale, are observed in the region above 900 cm^{-1} and in the range 650–250 cm^{-1}, respectively. Bands below 250 cm^{-1} are practically unchanged and bands in the spectral range from 900 to 700 cm^{-1} reveal shifts of only *ca.* 10 cm^{-1}. The results are comparable with ^{18}O-isotopic shifts described for NaZSM-5 in the far-[23] and mid-IR.[7]

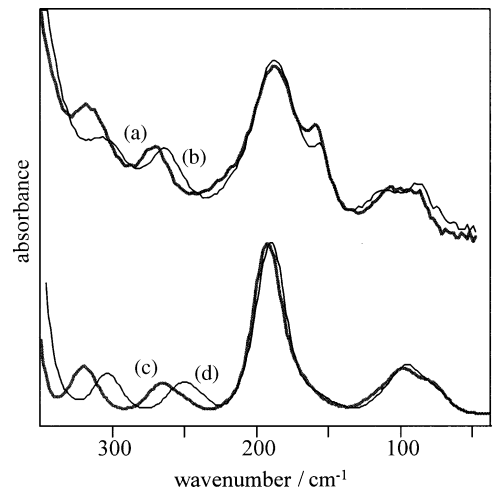

Fig. 3 Far-IR spectra: experimental NaY (a) and ^{18}O-NaY (b), shell model calculated NaY (c) and ^{18}O-NaY (d)

Calculated spectra

As described, two different methods were used to calculate vibrational spectra. Since geometry optimization is the first step in the shell model calculation procedure, the optimized geometry is compared with experimental data in Table 3, revealing a satisfying agreement. The calculated spectra are shown in Fig. 2 and 3. Wavenumbers of experimental and calculated bands are compared in Table 2. The far-IR region of the VFF calculation is not shown, since no cations were included in the calculation.

The overall agreement between experiment and both types of calculations is very satisfying and justifies the assumptions made in the calculations. The main characteristics are reproduced and the shifts on ^{18}O exchange in different spectral regions are in good agreement with experiment. However, the deviations of calculated wavenumbers from experiment are larger in the VFF calculations and the isotopic shift in the range 900–700 cm^{-1} is slightly overestimated. This is an indication that interaction force constants are not completely negligible. The largest shifts in the experiment, as well as in both

Table 2 Wavenumbers of experimental and calculated IR spectra of NaY (in cm^{-1})

experimental			shell model			valence force field		
^{16}O	^{18}O	$\Delta\tilde{\nu}$	^{16}O	^{18}O	$\Delta\tilde{\nu}$	^{16}O	^{18}O	$\Delta\tilde{\nu}$
1110 sh	1086	24	1096 vs	1055	41	1088 vs	1050	38
1033 vs	1000	33	1042 sh	993	49	900 w	869	31
797 w	787	10	838 m	834	4	798 m	779	19
727 b	717	10	722 b	717	5	677 w	653	24
587 w	571	16	595 w	577	18			
519 sh	502	17						
477 m	459	18	477 m	454	23	535 s	508	27
318 w	306	12	319 w	304	15			
272 w	264	8	265 w	250	15			
188 m	188	0	192 m	190	2			
159 sh	157	2						
100 m	98	2	98 w	95	3			

Table 3 Experimental and calculated geometry of sodium faujasite

	lattice parameter/Å	Si—O bond length (averaged)/Å	Al—O bond length (averaged)/Å	T—O—T angle/degrees
Shell model NaY	25.081	1.622	1.750	145.6
Eulenberger NaY[a]	24.71	T—O bond: 1.635		146.2
Olson NaX[b]	25.099	1.619	1.722	141.8

[a] Ref. 24; [b] ref. 14.

calculations, are found in the region above 900 cm^{-1} and in the range 650–250 cm^{-1}.

In order to gain a deeper insight into the vibrational behaviour, the common procedure for small molecules is visualization of their normal modes. As the 156 atoms in the unit cell give rise to $3N - 3 = 465$ normal modes the presentation of the individual normal modes proves to be not reasonable. The method of choice in this situation is the calculation of energy distributions.

In ionic models, *e.g.* the shell model, chemical bonds are taken into account only *via* bond-bending terms. In this case the computational procedures are performed in Cartesian coordinates and thus calculation of the KED is indicated. For each atom, the amplitude of the vibration is proportional to the velocity at the equilibrium position. Since the amplitudes of all atoms are given in eigenvectors, the kinetic energy is straightforwardly calculated as

$$T = \tfrac{1}{2}mv^2 \quad (6)$$

where m is the atomic mass and v is the velocity. The sum of the kinetic energies of all atoms during their motion is normalized to 100%. The KED for each normal mode, based on the shell model, is shown in Fig. 6 and 7 for the different types of atoms under study, as a function of wavenumbers. The KED of sodium ions is worthwhile mentioning only in the region below 250 cm^{-1}, indicating that a coupling between cation and framework modes can be neglected above 250 cm^{-1}. Thus, a discrimination between framework and cation modes can be made. Oxygen atoms have a very high share in the KED owing to the large number of oxygen atoms in comparison to the total number of atoms. More than 80% of the kinetic energy is concentrated on the oxygen atoms in the range 600–250 cm^{-1} and above 950 cm^{-1}. A minimum is clearly observed in the 900–700 cm^{-1} range. This is exactly the region in which the lowest shift due to ^{18}O exchange is obtained. Furthermore, the KED of oxygen shows a high contribution around 130 cm^{-1} (simultaneously a minimum for sodium) while the corresponding IR bands are of low intensities and therefore not observed in the spectra. Indications for such kinds of framework modes are discussed in the Raman spectra of zeolites.[25]

The displacements of silicon and aluminium atoms during the modes are in general rather small, probably due to the low flexibility of the T atom positions inside the zeolite lattice and the general T : O ratio of 1 : 2 in zeolites. Only the vibrations in the range 650–900 cm^{-1} show a more pronounced movement of T atoms, expressed by the maxima of the silicon KED at 850 cm^{-1} and of the aluminium KED around 700 cm^{-1}. These findings for aluminium are in agreement with the fact that an increased Si/Al ratio leads to a decrease in intensity of the bands at *ca.* 700 cm^{-1}.[26] Thus, a dominant influence of the aluminium displacements can be concluded in this range. The share of silicon is larger than for aluminium, owing to the presence of three times more silicon than aluminium atoms in the model.

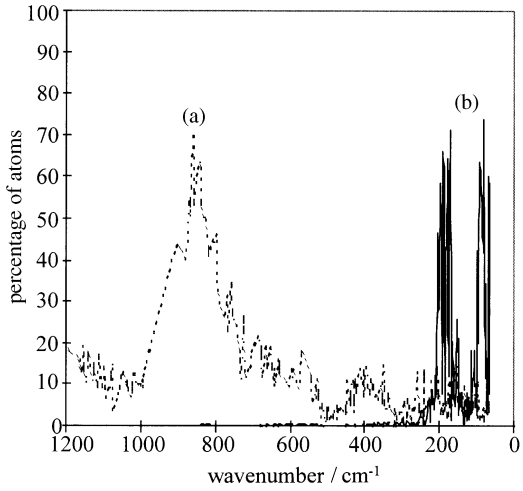

Fig. 6 Kinetic energy distribution of silicon atoms (a) and sodium ions (b) in NaY

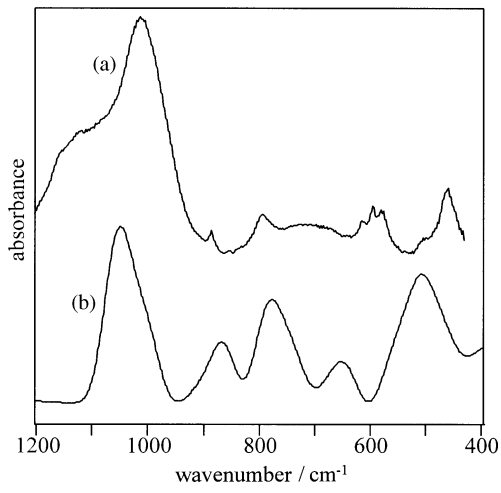

Fig. 5 Mid-IR spectrum of a high-temperature ^{18}O-exchanged NaY with lattice defects (a) and the VFF calculated spectrum (b)

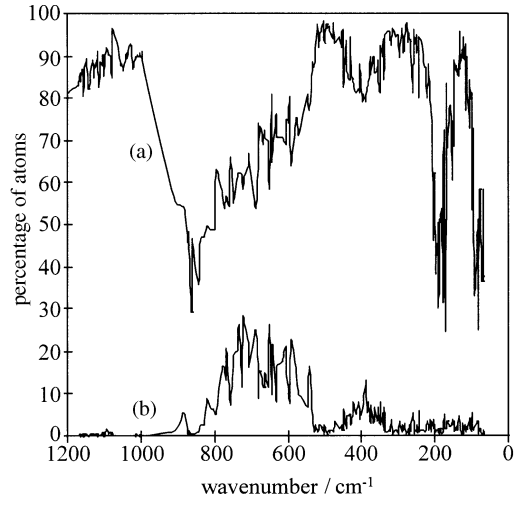

Fig. 7 Kinetic energy distribution of oxygen (a) and aluminium atoms (b) in NaY

The calculation of the PED is adequate in the case of a covalent force field model applying internal coordinates. The eigenvector is also given in internal coordinates and, since the potential expression for each internal coordinate is given by the force field, the potential energy and thus the PED are readily available for each normal mode k by

$$E^{(k)}_{\mathrm{p},ij} = F_{ij} L_{ik} L_{jk} \lambda_k^{-1} \quad \text{with} \quad \sum_j \sum_j E_{\mathrm{p},ij} = 1 \qquad (7)$$

where F_{ij} are the force constants ($i = j$ for diagonal ones), L_{ik} and L_{jk} are the elements of the eigenvector matrix and λ_k are the eigenvalues. The results of the PED calculation are similar to those of the KED. The region at *ca.* 1000 cm^{-1} shows a strong dominance, 70%, of Si—O bonds and only *ca.* 30% of Al—O bonds. The inverse holds in the region 700–800 cm^{-1}, where only 40% of the PED is concentrated on Si—O bonds and 60% is connected with Al—O bonds. A comparable effect was obtained in valence force field calculations for zeolite A.[27]

Furthermore, the PED shows that the additional band in the VFF spectrum at 900 cm^{-1} has to be assigned to stretching modes of terminal Si—O groups, as more than 80% of the potential energy is concentrated on these oscillators. On the one hand, this must be treated as model artefact for a perfect lattice owing to the absence of periodic boundary conditions. On the other, it leads to the important conclusion that the peak at 900 cm^{-1} in the experimental spectrum of high-temperature ^{18}O-exchanged faujasite, shown in Fig. 5, has to be explained by lattice defects. Another indication for defects is the additional bands at 614 and 595 cm^{-1}. The results obtained by the shell model show no bands at 900 cm^{-1} because of the use of periodic boundary conditions and the absence of terminal Si—O groups.

The calculations lead to the general conclusion that the bands above 950 cm^{-1} are caused by asymmetric vibrations of oxygen atoms in the TOT bridges and that the range 950–800 cm^{-1} has a strong participation of silicon atoms and the range 800–650 cm^{-1} of aluminium atoms. The spectral region 650–250 cm^{-1} is dominated by symmetric vibrations of oxygen atoms. This is in agreement with the very strong Raman band at 500 cm^{-1} which is assigned to a vibration where the oxygen atoms move along the T—O—T angle bisecting lines.[28] In this context, the relatively large ^{18}O shift of 16 cm^{-1} (Fig. 4) observed for this Raman band is not surprising. Bands below 250 cm^{-1} are mainly caused by cation vibrations coupled with low-frequency framework motions. Even if the distinction between framework and cation modes can be made in this way, a strong correlation between different cation sites and specific far-IR bands seems to be an oversimplification.[5,17]

Conclusions

Upon ^{18}O exchange, downscale shifts were observed in all vibrational spectra, whereas no additional bands occur. Interestingly, the extent of the isotopic shifts is different in different spectral regions and depends strongly on the nature of the normal modes. In this way, modes with significant displacements of oxygen atoms can be discriminated and thus it is possible to specify the vibrational assignment in the framework region. Assignments of the main absorptions are given on the basis of these experiments and calculations, whereas, in the case of the high-temperature ^{18}O-exchanged NaY, an additional band at 900 cm^{-1} was assigned to lattice defects. Bands below 250 cm^{-1}, being assigned to cation vibrations, show virtually no shift. Thus, by ^{18}O exchange, a discrimination between framework vibrations and vibrations with dominant cation displacements becomes feasible.

Both presented force fields and models are well suited for the description of the vibrational characteristics of NaY, including its ^{18}O-exchanged forms. However, the deviations from experiment are larger in the VFF calculations than in the shell model calculations indicating that the improvement of the VFF potential by parametrization of additional interaction force constants seems to be sensible. One possible method for the parametrization of these potentials is by using quantum mechanical calculations for small model clusters.[29] Alternatively, the number of experimental data in a fitting procedure for the force constants may be increased by isotopic substitution, as has been successfully applied for H/D exchange.[27] Although the lack of experimental data to fit the fine structure of force fields for zeolite frameworks cannot be removed by ^{18}O substitution alone, isotopic substitution of framework atoms seems to be of particular interest. Moreover, the physical relevance of a given force field can be confirmed by this procedure.

We gratefully acknowledge financial support by the Deutsche Forschungsgemeinschaft (Ge 783/1-2) and by the Graduiertenförderung der Universität Hamburg. We thank K-P. Schröder and J. Sauer of the Max-Planck-Gesellschaft, Berlin, for fruitful cooperation.

References

1 E. M. Flanigen, H. Khatami and H. A. Szymanski, *Adv. Chem. Ser.*, 1971, **101**, 201.
2 C. Brémard and M. Le Maire, *J. Phys. Chem.*, 1993, **97**, 9695.
3 C. R. A. Catlow, *Modelling of Structure and Reactivity in Zeolites*, Academic Press, London, 1992.
4 A. J. M. de Man and R. A. van Santen, *Zeolites*, 1992, **12**, 269.
5 K. Krause, E. Geidel, J. Kindler, H. Förster and K. Smirnov, *Vib. Spectrosc.*, 1996, **12**, 45.
6 R. von Ballmoos, *The ^{18}O-Exchange Method in Zeolite Chemistry*, Otto Salle Verlag, Frankfurt, 1981.
7 F. Bauer, E. Geidel, Ch. Peuker and W. Pilz, *Zeolites*, 1996, **17**, 278.
8 S. C. Parker, C. R. A. Catlow and A. N. Cormack, *Acta Crystallogr. B.*, 1984, **40**, 200.
9 B. G. Dick and A. W. Overhauser, *Phys. Rev.*, 1958, **112**, 90.
10 M. J. L. Sangster and M. Dixon, *Adv. Phys.*, 1976, **25**, 247.
11 B. Winkler and M.T. Dove, *Am. Mineral.*, 1991, **76**, 313.
12 K-P. Schröder and J. Sauer, *J. Phys. Chem.*, 1996, **100**, 11043.
13 *Catalysis User Guide*, version R-4.0, San Diego: Biosym Technologies, 1993.
14 D. H. Olson, *Zeolites*, 1995, **15**, 439.
15 J. A. Creighton, H. W. Deckman and J. M. Newsam, *J. Phys. Chem.*, 1994, **98**, 448.
16 A. J. M. de Man, B. W. H. van Beest, M. Leslie and R. A. van Santen, *J. Phys. Chem.*, 1990, **94**, 2524.
17 K. Krause, E. Geidel, J. Kindler, H. Förster and H. Böhlig, *J. Chem. Soc., Chem. Commun.*, 1995, 2481.
18 E. B. Wilson, Jr., J. C. Decius and P. C. Cross, *Molecular Vibrations*, McGraw-Hill, New York, 1955.
19 R. N. Jones, *Computer Programs for Infrared Spectrophotometry—Normal Coordinate Analysis*, NRCC Bulletin No. 15, Canada, 1976.
20 C. S. Blackwell, *J. Phys. Chem.*, 1979, **83**, 3251; 3257.
21 E. Geidel, H. Böhlig, Ch. Peuker and W. Pilz, *Stud. Surf. Sci. Catal.*, 1991, **65**, 511.
22 E. Geidel, H. Böhlig and P. Birner, *Z. Phys. Chem.*, 1991, **171**, 121.
23 H. Esemann, K. Krause, E. Geidel and H. Förster, *Microporous Mater.*, 1996, **6**, 321.
24 G. R. Eulenberger, D. P. Shoemaker and J. G. Keil, *J. Phys. Chem.*, 1967, **71**, 1812.
25 C. Brémard and D. Bougeard, *Adv. Mater.*, 1995, **7**, 10.
26 P. Pichat, R. Beaumont and D. Barthomeuf, *J. Chem. Soc., Faraday Trans. 1*, 1974, **70**, 1402.
27 M. Bärtsch, P. Bornhauser, G. Calzaferri and R. Imhof, *J. Phys. Chem.*, 1994, **98**, 2817.
28 F. L. Galeener, *Phys. Rev. B*, 1979, **19**, 4292.
29 V. A. Ermoshin, K. S. Smirnov and D. Bougeard, *Chem. Phys.*, 1996, **202**, 53; 1996, **209**, 41.

Paper 6/06253I; *Received* 10*th September*, 1996